Classical model of two electrons interacting in a saddle-shaped electric potential, and a constant perpendicular magnetic field

Ruhaan Bhargav

Beanstalk International Bilingual School, Beijing, China

Abstract. Electron collisions are fundamental phenomena in modern physics with diverse applications ranging from collision ionization to quantum computing and high-energy plasma studies. This paper focuses on the intricate dynamics of electron collisions within a saddle-shaped electric potential and a constant magnetic field, mimicking the conditions found in beam splitters (and particle accelerators). While existing studies often employ a quantum framework to model these interactions and actually perform the experiment, we adopt a classical approach to provide a more intuitive understanding of the phenomena involved. The transition from quantum to classical representation eliminates probabilistic elements, allowing for precise and deterministic simulations. We utilized a self-programmed python script based on mathematical expressions for the situation, which are also self-derived in the paper. We have managed to replicate 2/4 results simply by altering the starting positions of the electrons and have added further functionality within the python simulations for further research and development i.e., a softening factor controlling the relative screening effect of the material of the constriction, and a time delay feature to be able to offset the starting time of one of the particles relative to the other. Our hope with this paper is for people to be able to take our results, and the model used to derive them, and use it for the purposes of further research and exploration.

Keywords: saddle-shaped electric potential, perpendicular magnetic field, Electron collisions.

1. Introduction

Electron collisions play a very important role in modern physics. This phenomenon can be utilized in various scenarios such as collision ionization [1], cubit encoding [2], and low energy plasma [3]. While low energy collisions have been replicated several times, and are utilized at a regular basis [4][5][6], high-energy electron collisions are not as common an occurrence. In order for the like-charged particles (electrons) to collide with one another, electromagnetic particle accelerators are required; these not only accelerate the particles, but also need to counter-act the opposing forces which exist between them. Therefore, the particle accelerators generally used in beam splitters and other similar devices must be capable of accelerating electrons to a high enough energy to allow for a Coulomb collision between the electrons while negating the screening effects of the medium [7]. Furthermore, it is not simply the ability to collide two electrons/charged particles but use these Coulomb interactions to create beams/flow of charges or particles is crucial technology in a wide range of scientific and technological fields; from radiation therapy[11] to microscopy[12] and lithography[13], beam splitting, especially of charged particles. Overall, these collisions play a pivotal role in understanding the behavior of subatomic particles and the fundamental forces which shape our universe. The electrical field inside a beam splitter does the job of accelerating the electrons towards each other against the opposing Coulomb force of the other electron. In a lot of cases where the particles aren't accelerated to a high degree, the electric field must also be shaped to compensate for the screening-effect of the medium in which the collision is taking place. In the case of our experiment, which further aims to replication real world tests of high energy electron beam splitting[7][9], the electric field of choice is of a saddle shaped. The saddle shape allows the electrons from almost any variable starting position and energy level to approach the central co-ordinates (0,0) in reference to the potential. Since our aim is to interact two like-charged particles, making the saddle-shape of the potential very important in bringing the two electrons together from symmetrical starting positions. As the model, just like the experiment, aims to target the electrons towards a central point,

a saddle shaped potential is the most consistent way to do so. Since the electrons are repelling against one another, and the saddle shaped potential is taking the electrons through a curved path to accelerate them towards one another, the magnetic field is used to cancel out, or even rotate the electrons towards one another. A magnetic field on a moving charge has the same effect as a gravitational field to a moving mass, it adds angular acceleration to the charge. Since the a combination of the saddle shaped potential and Coulomb interaction would distribute the electrons away from one another, the constant magnetic field forces the electrons to rotate towards the center of the collider constriction.

High energy wave-packet colliders, and charged particle beam splitters all utilize an electric potential and magnetic fields in order to drive the electrons close enough for Coulomb interactions. Existing studies model these interactions within a quantum framework [7][9], getting results which follow the experimentally verified probability distributions. While doing so provides an accurate model for predictions, it may not, however, provide an intuitive understanding of the subject. With this study, we aim to model these interactions within beam splitter using a classical framework to understand and visualize what is happening at the atomistic scale. Transitioning from a quantum framework to a classical one removes the probabilistic element of the collision. Just like the wave-like nature of the electron, a quantum framework would comprise of more outcomes than a simple classical simulation. A classical interaction with the exact same parameters would naturally have the exact outcome in both theory and reality [15], while the quantum reality of the phenomenon ensures an element of randomness in the context of the experiment. The electron, rather than a point-like particle in a classical framework, would be a probability-wave of positions. This means that in every trial, the electrons exists in a superposition with the peak of the probability wave at the starting position. While doing so provides a more accurate representation of the real outcomes of the experiment, the electrons can also be modelled to have a variable starting position in a classical framework. In order to mimic the quantum nature of electrons, while also maintaining a visual and understandable classical model.

In this paper, we will alter the starting positions of the electrons in the classical model to then replicate the quantum experimental results [7][9]. With the aim to explore and model electron collisions within a saddle-shaped electric potential, and constant magnetic field, simulating the real conditions inside a beam splitter using a classical framework. Our primary focus is ultimately to contribute to the advancement of knowledge in the field of electron collisions and the ability to have an intuitive understanding of the phenomenon.

2. Formalism

2.1. Coulomb Collision

In order to successfully create a classical simulation modelling the motion of two electrons within a complex system, one of the first interactions which needs to be resolved is the Coulomb interaction between the two charged particles. Coulomb collisions are binary elastic collision between 2 charged particles through their own electric fields *(Insert Reference)*. As the name suggests, these collisions are based on the Coulomb inverse square law, and formalize how the separate fields of the 2 charged particles (in our case, electrons) would interact classically and produce ideal elastic collisions. An ideal Coulomb interaction between 2 electrons is represented as

$$U_C(\vec{r_1}, \vec{r_2}) = \frac{e^2}{4\pi\epsilon_0\epsilon_r}\left(\frac{1}{|\vec{r_1} - \vec{r_2}|}\right) = \frac{e^2}{4\pi\epsilon_0\epsilon_r\sqrt{(x_1 - x_2)^2 + (y_1 - y_2)^2}}: \quad (1)$$

Where $\vec{r_1}$ and $\vec{r_2}$ mark the positions of the electrons; *e* is the elementary charge of the electron; ϵ_0 is the permittivity of free space, and ϵ_r is the relative permittivity of whatever medium the experiment is conducted in. Visualizing this interaction without any other forces involved results in the following trajectories (Fig. 1):

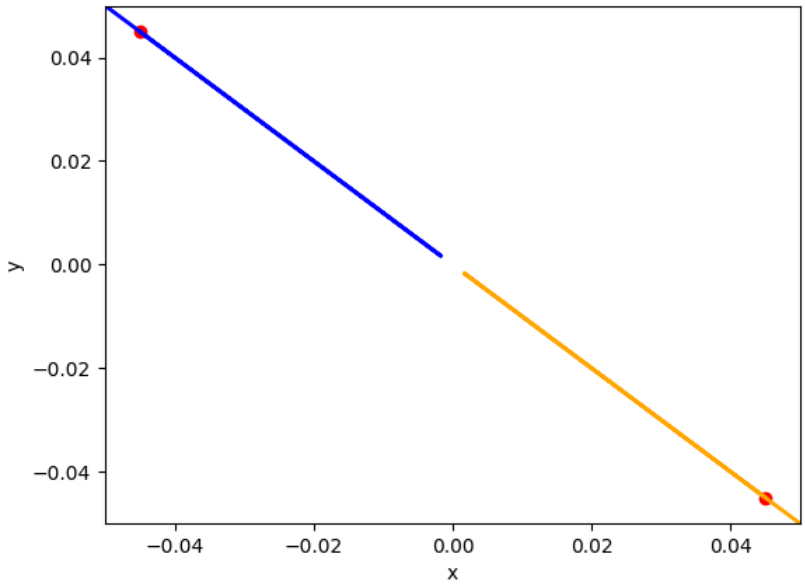

Figure 1. *Conditions – Starting co-ordinates: (0.045, -0.045) and (-0.045, 0.045); Electric and Magnetic field strength = 0; Permittivity of free space and relative permittivity = 1; Charge of electron (e) = -1*

However, even without the presence of an electric or magnetic field, a realistic experiment colliding 2 charged particles in any medium would experience what is known as "screening". Due to the structure of the material that is the medium, and the existence of charged particles which are relatively large in context to the electrons, the pure Coulomb interaction between the 2 particles is "screened" by the material itself. Because this screening effect is a result of the Coulomb interaction between the material and the electrons, a small factor can be used to modify (1) to account for the screening. With a new variable $S_{screening}$ representing a softening factor for the Coulomb interaction caused by the screening effect, we have

$$U_C(\vec{r_1},\vec{r_2}) = \frac{e^2}{4\pi\epsilon_0\epsilon_r}\left(\frac{1}{|\vec{r_1}-\vec{r_2}|} - \frac{1}{[(\vec{r_1}-\vec{r_2})^2 + S_{screening}]^{\frac{1}{2}}}\right): \tag{2}$$

Where $S_{screening}$ is proportional to the distance between the 2 detectors in the experiment, or the size of our reference frame in the simulation.

2.2. Saddle Potential

In order to accelerate the electrons towards each other with a Coulomb interaction already present between the two electrons; there exists an electric field. This electric field, in order to compensate for the repulsive nature of the coulomb interaction, cannot be linear with respect to the co-ordinate system. Rather, just like the experiments, we have modelled a saddle-shaped electric potential *Insert Reference* represented as

$$U_{saddle}(x,y) = -\frac{1}{2}\omega_x^2 x^2 + \frac{1}{2}\omega_y^2 y^2, \tag{3}$$

Where ω_x and ω_y are the frequencies describing the curvature of the barrier potential. The potential is being described through its frequency related factors ω_x and ω_y primarily due to the harmonic nature of this potential: in fact, the frequency factors are directly related to the harmonic-oscillating behavior a charged particle would exhibit in this saddle-shaped potential. On the contrary, the constants can be easily visualized as mere factors to the individual quadratics that exist in the *x* and *y* axes independently. We can visualize this potential as a surface plot for conditions $\omega_x = \omega_y = 1$ as shown in Fig. 2:

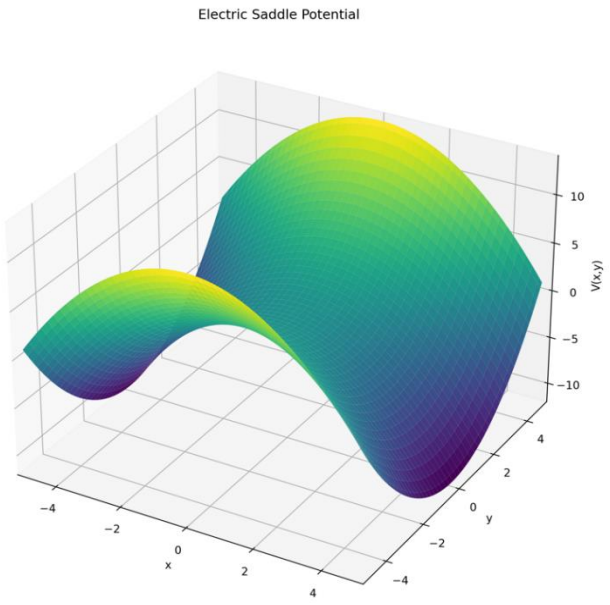

Figure 2. (a)

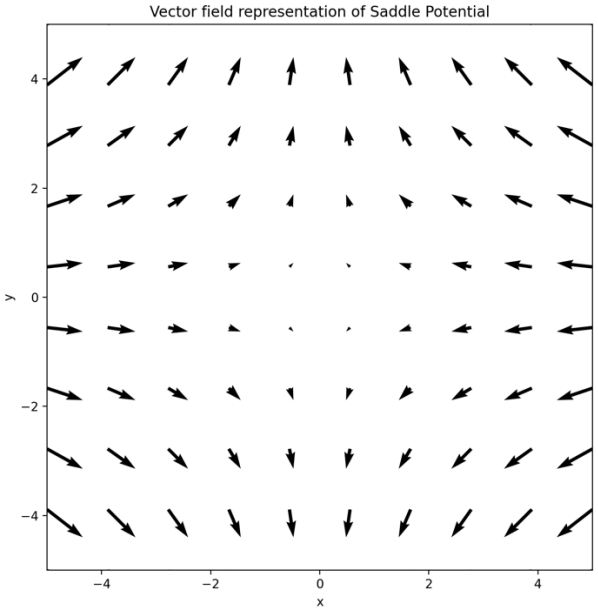

Figure 2. (b)

Figure 2. *(a) Is a surface plot of the potential of the above defined electric field: high values represented by lighter colors, and smaller values represented by darker colors? (b) Is a vector field of the same potential; where the vectors represent the force experienced by a positive charge within the field.*

While the actual values for the constants will be derived later in section 3.2, there are certain relationships which exist in past experiments and must be replicated. Due to the nature of the scale of our model, this collision can be classified as occurring in a moderate to wide constriction: in which, the electric field would be such that $\frac{\omega_x}{\omega_y} \geq 1$ [14]. For the case of our model, an effective approximation such that $\frac{\omega_x}{\omega_y} = 1$ would suffice.

Since $\omega_x = \omega_y$, our initial saddle-potential is a good approximation of the actual electric field in the experiment and model; therefore, can be utilized in order to visualize the paths of the charged particles without other interference. In Fig. 3, the colored lines show the equipotential trajectories of individual electrons on the horizontal plane representing the 2 spatial dimensions, and the height representing the potential at which they are travelling.

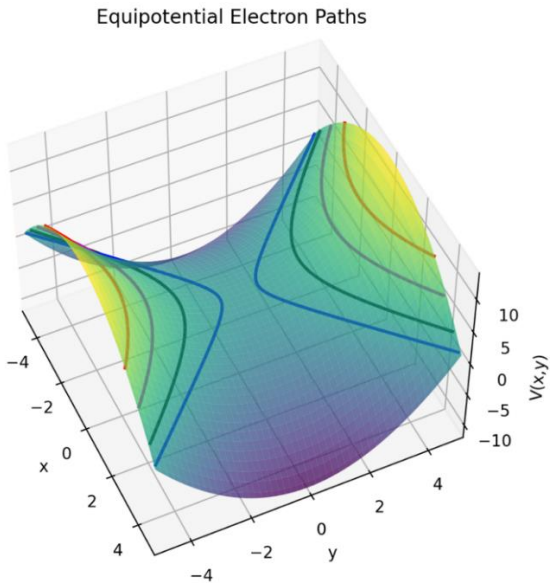

Figure 3. *Each color line individually represents a unique potential value, and the lines themselves are all points on the surface where the potential stays constant at that specific value*

These trajectories of constant potential were calculated simply using (3)

$U_{saddle}(x, y) = C$

$$\frac{1}{2}\omega_y^2 y^2 = \frac{1}{2}\omega_x^2 x^2 + C$$

$$y = \pm\sqrt{\frac{\omega_x^2}{\omega_y^2}x^2 + \frac{C}{\omega_y^2}}$$

Where C is any potential for which $U_{saddle}(x,y) = C$ holds true.

2.3. The Lorentz Force

Now having covered both the Coulomb interaction between the two particles, alongside the saddle potential of the electric field, the last remaining component of the experiment to be considered is the constant magnetic field. Throughout the experiment, there will be a constant magnetic field acting on both our electrons $\vec{B} = \begin{bmatrix} 0 \\ 0 \\ B \end{bmatrix}$. In order to incorporate the effect of this magnetic field,

We used the Lorentz Force to further formalize its relationship to the velocities, and therefore, the positions of the particles. The Lorentz Force is represented by

$\overrightarrow{F_{Lorentz}} = q\,(\vec{E} + \vec{v} \times \vec{B})$

Where $\vec{F}_{Lorentz}$ is the force experienced by a charged particle with charge q, and velocity $\vec{v}$ within an electric field $\vec{E}$ and magnetic field$\vec{B}$? In practical terms, this equation demonstrates that the force experienced by a point charge q is a combination of the force in the direction of the Electric field$\vec{E}$, and proportional to the magnitude of the electric field and the quantity of charge, and the force perpendicular to the direction of the Magnetic field $\vec{B}$ and velocity $\vec{v}$ of the charge, and proportional to the strength of the magnetic field, magnitude of the velocity, and charge of the point particle [10].

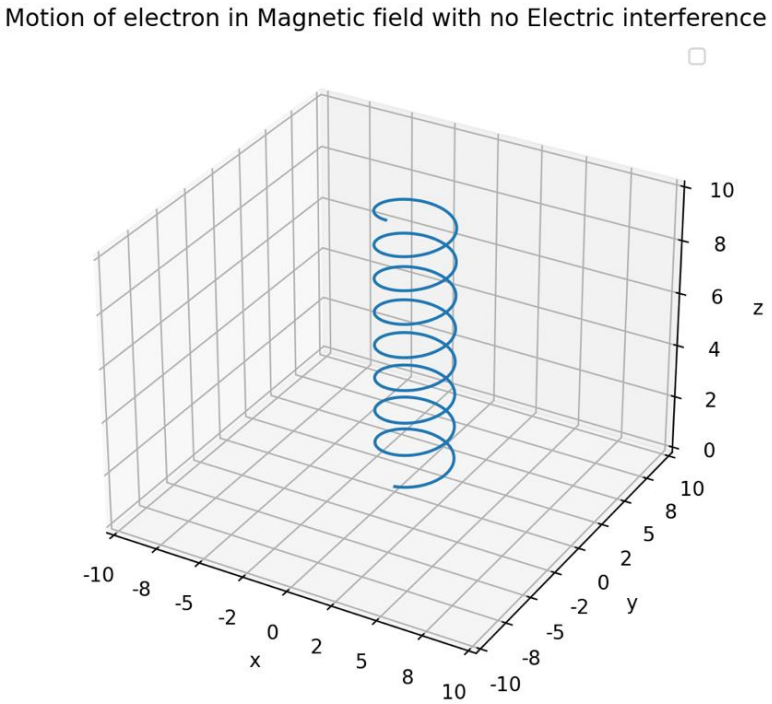

Figure 4. *Path of an electron in a constant magnetic field and an initial velocity of 10 units in the z-direction.*

As seen in Fig. 4, the effect of a magnetic field $\vec{B}$ (As defined above), on a charged particle without the existence of an electric field results in a harmonic circular motion (In the figure, the

trajectory is a helix due to the initial velocity of the particle). Meaning that similar to factors ω_x and ω_y representing the electric field, a similar frequency factor ω_c or the "Cyclotron Resonance Frequency" can be used to describe the magnetic field.

The Cyclotron Resonance Frequency is simply the frequency of a charged particle moving perpendicular to the direction of a uniform magnetic field *B*. By definition, this motion must be circular, and can therefore be represented through an equality of the Lorentz force and centripetal acceleration [8]. Equating the magnitudes of the forces in our case:

$$\frac{mv^2}{r} = qBv$$

$$\frac{v}{r} = \frac{qB}{m}$$

Since $\frac{v}{r} = \omega_c$,

$$\omega_c = \frac{q}{m}B$$

$$\omega_c \propto B$$

Therefore, we can define a new constant ω_c, such that:

$$\vec{B} = \begin{bmatrix} 0 \\ 0 \\ B \end{bmatrix} = \begin{bmatrix} 0 \\ 0 \\ \omega_c \end{bmatrix} \tag{4}$$

Transforming our vector fields to accommodate for this magnetic field for each of the 2 electrons based on their starting velocities results in Fig. 5

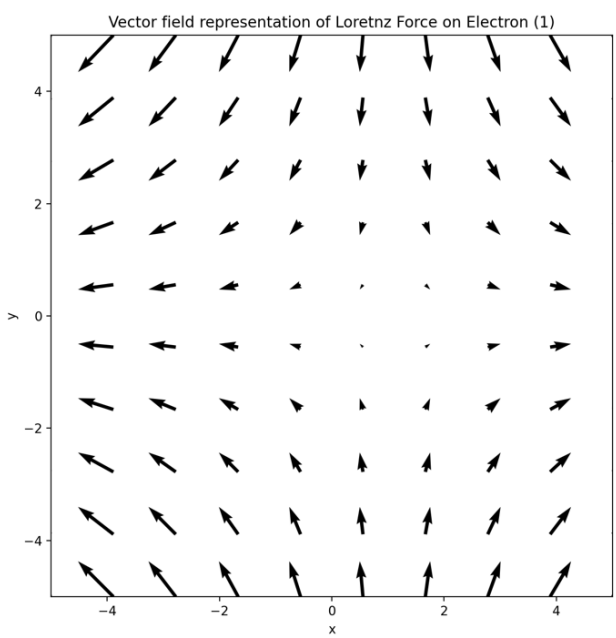

Figure 5. (a)

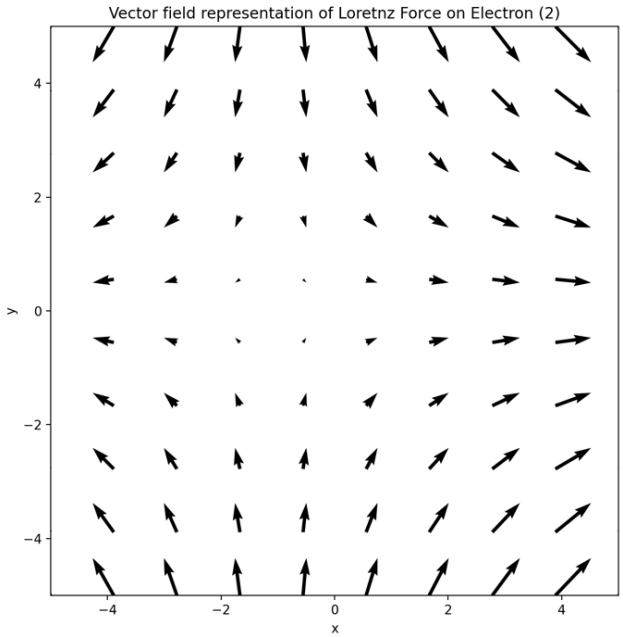

Figure 5. (b)

Figure 5. *The force experienced by positive charges 1 (a) and 2 (b) in a constriction with both an electric saddle potential and constant magnetic field. The difference in the 0-point for these fields occurs due to the difference in the direction of their caused by a difference in starting position and the requirement of the electrons to be fired towards one another.*

Fig. 5(a) models the motion of a positive charge with a constant velocity (-1, 1), and therefore curves shown must be reversed to understand the motion of an electron with the same velocity. In this case, the resultant curvature would be counter-clockwise instead of the clockwise seen in the figure. Similarly, Fig. 5(b) models the motion of a positive charge with a constant velocity (1,-1), and the centripetal path of the electron would be clockwise rather than the counter-clockwise as seen in the image.

3. Methodology

3.1. The Equations

In order to model the motion of 2 electrons inside an electric saddle potential U_{saddle}, and a constant magnetic field $\vec{B}$ mechanically, we need to evaluate all the forces acting on both the electrons within our system. In our case, the forces acting on particle-1 and particle-2 will be evaluated separately such that:

$$\vec{F_1} = \vec{F_1^\circ} + \vec{F_1^B} \tag{5}$$

$$\vec{F_2} = \vec{F_2^\circ} + \vec{F_2^B} \tag{6}$$

Where $\vec{F_{1,2}^\circ}$ the force is experienced due to the saddle-shaped Electric Field and Coulomb interaction between the particles, and $F_{1,2}^B$ is the Lorentz force experienced due to the constant Magnetic field $\vec{B} = \begin{bmatrix} 0 \\ 0 \\ \omega_c \end{bmatrix}$.

3.1.1. Solving for $\vec{F_{1,2}^\circ}$

From 2.2, we know that:

$U_{saddle} = \frac{1}{2}\omega_y^2 y^2 - \frac{1}{2}\omega_x^2 x^2$.

Since the Coulomb interactions, which must also be modelled under $\vec{F}^\circ$ (Since it is an electric interaction), can also be represented in terms of a potential $U_{coulomb}$ from 2.1 where:

$U_{coulomb} = \frac{e^2}{|\vec{r_1} - \vec{r_2}|} = \frac{e^2}{\sqrt{(x_1 - x_2)^2 + (y_1 - y_2)^2}}$.

We can now utilize the definition of a Potential: $F = \frac{-dU}{dx}$ in order to evaluate $\vec{F}^\circ$. In the case of our model, the variable: $\vec{F}^\circ$ must be simplified into its components and solved independently for particle 1 and 2 (Note: x and y represent the position of the particle with respect to our defined frame of reference) such that:

$$\vec{F_1^\circ} = \begin{bmatrix} F_{1x}^\circ \\ F_{1y}^\circ \\ 0 \end{bmatrix} = \begin{bmatrix} -\frac{\partial U_{tot}}{\partial x_1} \\ -\frac{\partial U_{tot}}{\partial y_1} \\ 0 \end{bmatrix} \tag{7}$$

$$\vec{F_2^\circ} = \begin{bmatrix} F_{2x}^\circ \\ F_{2y}^\circ \\ 0 \end{bmatrix} = \begin{bmatrix} -\frac{\partial U_{tot}}{\partial x_2} \\ -\frac{\partial U_{tot}}{\partial y_2} \\ 0 \end{bmatrix} \tag{8}$$

Where *Utot = Usaddle + Ucoulomb* such that:

$$U_{tot} = -\frac{1}{2}\omega_x^2 x_1^2 - \frac{1}{2}\omega_x^2 x_2^2 + \frac{1}{2}\omega_y^2 y_1^2 + \frac{1}{2}\omega_y^2 y_2^2 + \frac{e^2}{\sqrt{(x_1 - x_2)^2 + (y_1 - y_2)^2}} \tag{9}$$

The next step is to evaluate the partial derivatives and calculate an exact expression for the Forces $\vec{F}^{\circ}_1$ and $\vec{F}^{\circ}_2$. Utilizing (7) and (8), we have:

$$F^{\circ}_{1x} = -\frac{\partial U_{tot}}{\partial x_1} = \omega_x^2 x_1 + \frac{e^2(x_1 - x_2)}{((x_1 - x_2)^2 + (y_1 - y_2)^2)^{\frac{3}{2}}}$$

$$F^{\circ}_{1y} = -\frac{\partial U_{tot}}{\partial y_1} = -\omega_y^2 y_1 + \frac{e^2(x_1 - x_2)}{((x_1 - x_2)^2 + (y_1 - y_2)^2)^{\frac{3}{2}}}$$

$$F^{\circ}_{2x} = -\frac{\partial U_{tot}}{\partial x_2} = \omega_x^2 x_2 - \frac{e^2(x_1 - x_2)}{((x_1 - x_2)^2 + (y_1 - y_2)^2)^{\frac{3}{2}}}$$

$$F^{\circ}_{2y} = -\frac{\partial U_{tot}}{\partial y_2} = -\omega_y^2 y_2 - \frac{e^2(x_1 - x_2)}{((x_1 - x_2)^2 + (y_1 - y_2)^2)^{\frac{3}{2}}}$$

Which allows to conclude:

$$\vec{F^{\circ}_1} = \begin{bmatrix} \omega_x^2 x_1 + \frac{e^2(x_1 - x_2)}{((x_1 - x_2)^2 + (y_1 - y_2)^2)^{\frac{3}{2}}} \\ -\omega_y^2 y_1 + \frac{e^2(x_1 - x_2)}{((x_1 - x_2)^2 + (y_1 - y_2)^2)^{\frac{3}{2}}} \\ 0 \end{bmatrix} \tag{10}$$

$$\vec{F^{\circ}_2} = \begin{bmatrix} \omega_x^2 x_2 - \frac{e^2(x_1 - x_2)}{((x_1 - x_2)^2 + (y_1 - y_2)^2)^{\frac{3}{2}}} \\ -\omega_y^2 y_2 - \frac{e^2(x_1 - x_2)}{((x_1 - x_2)^2 + (y_1 - y_2)^2)^{\frac{3}{2}}} \\ 0 \end{bmatrix} \tag{11}$$

3.1.2. Solving for F^B

From 2.3, we know that the effect of a constant magnetic field and electric field (which in our case is represented as $\vec{B} = \begin{bmatrix} 0 \\ 0 \\ \omega_c \end{bmatrix}$) on a charged particle can be modeled using the equation:

$\overrightarrow{F_L} = q\vec{E}_0 + q\,(\vec{v} \times \vec{B})$

Since we have already modelled the effect of $q\vec{E}_0$ as $\vec{F}^{\circ}$, we only need to compute for $q(\vec{v} \times \vec{B})$ as the equivalent expression for $\vec{F}^B$. Once again, this computation needs to be carried out for the 2 different particles and factored into a final expression for the force. From this point forwards, we will be using the substitution $q = e$, where q is the charge of any particle and e is the charge of an electron (Since the model is based on electron collisions).

$$\vec{F_1^B} = e(\vec{v_1} \times \vec{B}) \tag{12}$$

$$\vec{F_2^B} = e(\vec{v_2} \times \vec{B}) \tag{13}$$

Expanding (12)

$$e(\vec{v_1} \times \vec{B}) = e \begin{bmatrix} v_{1x} \\ v_{1y} \\ v_{1z} \end{bmatrix} \times \begin{bmatrix} 0 \\ 0 \\ \omega_c \end{bmatrix}$$
$$= e \begin{bmatrix} i & j & k \\ v_{1x} & v_{1y} & v_{1z} \\ 0 & 0 & \omega_c \end{bmatrix}$$

Therefore

$$\vec{F_1^B} = e(\vec{v_1} \times \vec{B}) = \begin{bmatrix} ev_1 y\omega_c \\ -ev_1 x\omega_c \\ 0 \end{bmatrix} \tag{14}$$

The same process follows for (13)

$$e(\vec{v_2} \times \vec{B}) = e \begin{bmatrix} v_{2x} \\ v_{2y} \\ v_{2z} \end{bmatrix} \times \begin{bmatrix} 0 \\ 0 \\ \omega_c \end{bmatrix}$$
$$= e \begin{bmatrix} i & j & k \\ v_{2x} & v_{2y} & v_{2z} \\ 0 & 0 & \omega_c \end{bmatrix}.$$

Therefore

$$\vec{F_2^B} = e(\vec{v_2} \times \vec{B}) = \begin{bmatrix} ev_{2y}\omega_c \\ -ev_{2x}\omega_c \\ 0 \end{bmatrix} \tag{15}$$

3.1.3. Final expressions

Since we now have the mathematical expressions for $\vec{F_1^\circ}$, $\vec{F_2^\circ}$, $\vec{F_1^B}$, and $\vec{F_2^B}$ in (10), (11), (14), and (15) Respectively. We can utilize our main relationship (5) in order to derive an expression for the force acting on both of our electrons independently.

$$\vec{F_1} = \vec{F_1^{\circ}} + \vec{F_1^{B}} = \begin{bmatrix} \omega_x^2 x_1 + \frac{e^2(x_1-x_2)}{((x_1-x_2)^2+(y_1-y_2)^2)^{\frac{3}{2}}} \\ -\omega_y^2 y_1 + \frac{e^2(y_1-y_2)}{((x_1-x_2)^2+(y_1-y_2)^2)^{\frac{3}{2}}} \\ 0 \end{bmatrix} + \begin{bmatrix} ev_{1y}\omega_c \\ -ev_{1x}\omega_c \\ 0 \end{bmatrix}$$

$$\vec{F_2} = \vec{F_2^{\circ}} + \vec{F_2^{B}} = \begin{bmatrix} \omega_x^2 x_2 - \frac{e^2(x_1-x_2)}{((x_1-x_2)^2+(y_1-y_2)^2)^{\frac{3}{2}}} \\ -\omega_y^2 y_2 - \frac{e^2(x_1-x_2)}{((x_1-x_2)^2+(y_1-y_2)^2)^{\frac{3}{2}}} \\ 0 \end{bmatrix} + \begin{bmatrix} ev_{2y}\omega_c \\ -ev_{2x}\omega_c \\ 0 \end{bmatrix}$$

Since $\vec{F} = m\vec{a} = m\dot{\vec{v}} = m\begin{bmatrix} \dot{v_x} \\ \dot{v_y} \\ \dot{v_z} \end{bmatrix}$, we can equate the above relationships in order to derive the Equations of motion for the 2 particles:

$$\vec{F_1} = \begin{bmatrix} \omega_x^2 x_1 + \frac{e^2(x_1-x_2)}{((x_1-x_2)^2+(y_1-y_2)^2)^{\frac{3}{2}}} + ev_{1y}\omega_c \\ -\omega_y^2 y_1 + \frac{e^2(y_1-y_2)}{((x_1-x_2)^2+(y_1-y_2)^2)^{\frac{3}{2}}} - ev_{1x}\omega_c \\ 0 \end{bmatrix},$$

$$\vec{F_2} = \begin{bmatrix} \omega_x^2 x_2 - \frac{e^2(x_1-x_2)}{((x_1-x_2)^2+(y_1-y_2)^2)^{\frac{3}{2}}} + ev_{2y}\omega_c \\ -\omega_y^2 y_2 - \frac{e^2(x_1-x_2)}{((x_1-x_2)^2+(y_1-y_2)^2)^{\frac{3}{2}}} - ev_{2x}\omega_c \\ 0 \end{bmatrix}.$$

In order to utilize these equations for the purposes of modelling motion in python, we need to convert the acceleration into a velocity through finite differences. For the purposes of writing out the equation, we will use the *f*(*x*) notation of functions and Δ*t* to represent the finite difference, as we are not taking the differentiating limit:

$$\begin{bmatrix} \dot{v_x} \\ \dot{v_y} \\ \dot{v_z} \end{bmatrix} = \begin{bmatrix} \frac{\Delta v_x}{\Delta t} \\ \frac{\Delta v_y}{\Delta t} \\ \frac{\Delta v_z}{\Delta t} \end{bmatrix} = \begin{bmatrix} \frac{v_x(t+\Delta t)-v_x(t)}{\Delta t} \\ \frac{v_y(t+\Delta t)-v_y(t)}{\Delta t} \\ \frac{v_z(t+\Delta t)-v_z(t)}{\Delta t} \end{bmatrix}.$$

Therefore (Note* $v_z = 0$):

$$v_{1x}(t+\Delta t) = \Delta t(\omega_x^2 x_1(t) + \frac{e^2(x_1(t)-x_2(t))}{((x_1(t)-x_2(t))^2+(y_1(t)-y_2(t))^2)^{\frac{3}{2}}} + ev_{1y}(t)\omega_c) + v_1 x(t), \quad (16)$$

$$v_{1y}(t+\Delta t) = \Delta t(-\omega_y^2 y_1(t) + \frac{e^2(y_1(t)-y_2(t))}{((x_1(t)-x_2(t))^2+(y_1(t)-y_2(t))^2)^{\frac{3}{2}}} - ev_{1x}(t)\omega_c) + v_1 y(t), \quad (17)$$

$$v_{2x}(t+\Delta t) = \Delta t(\omega_x^2 x_2(t) - \frac{e^2(x_1(t)-x_2(t))}{((x_1(t)-x_2(t))^2+(y_1(t)-y_2(t))^2)^{\frac{3}{2}}} + ev_{2y}(t)\omega_c) + v_2 x(t), \quad (18)$$

$$v_{2y}(t+\Delta t) = \Delta t(-\omega_y^2 y_2(t) - \frac{e^2(x_1(t)-x_2(t))}{((x_1(t)-x_2(t))^2+(y_1(t)-y_2(t))^2)^{\frac{3}{2}}} - ev_{2x}(t)\omega_c) + v_2 y(t), \quad (19)$$

Where:

$$x(t) = v_x(t)\Delta t + x(t-\Delta t)$$
$$y(t) = v_y(t)\Delta t + y(t-\Delta t)$$

3.2. Determining the constants

In order to construct an accurate model for the real experiments, the value of certain constants must be held as constant. Some of these values include the ω values including ω_x, ω_y, and ω_z as they parameterize the electric and magnetic fields under the influence of which the electrons will move through the whole apparatus.

Due to the scale of the experiment and constriction through which the electrons will pass, the relationship between ω_x and ω_y would be such that $\frac{\omega_x}{\omega_y} = 1$. Due to the nature of the simulation, all values are merely in proportional relationship to one another, where $e = -1$ (Charge of 1 electron), $m = 1$ (Effective mass), the size of the constriction is 0.05, and $DT = 0.00005$ (The finite difference). Similarly, in order to maintain simplicity and the symmetry in the saddle potential, we have set $\omega_x = \omega_y = 1$. Due to this, the shape and proportionality of the potential would be exactly equivalent to the potential as proposed in section 2.2.

Aside from the exact numerical value assigned to ω_x and ω_y, first a relationship, and then a value needs to be assigned to ω_c. According to the experimental setup of "*Two electrons interacting at a mesoscopic beam splitter*" [7], the relationship between ω_c and ω_y such that:

$$\frac{\omega_c}{\omega_x} = \frac{17.5\ meV}{1.7\ meV} \quad (20)$$

$$\frac{\omega_c}{\omega_x} \approx \frac{10}{1} \quad (21)$$

Using this as a starting point, we simulated the trajectories of the electron through an Electromagnetic field represented by $\omega_x = \omega_y = 1$ and $5 \leq \omega_c \leq 10$ (with increments of 1) until a relatively stable magnetic field strength was found. Fig.6 are the results of the simulated behavior, and it is the general similarity of the electron trajectory to the reference material which lead to the decision of using $\omega_c = 9$:

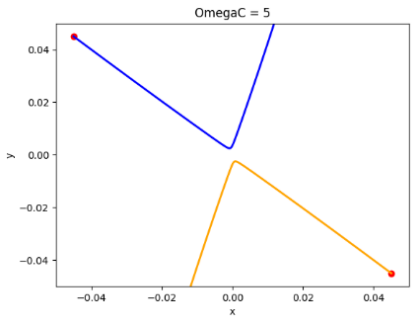

Figure 6. (a)

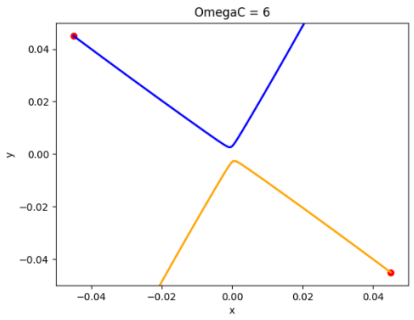

Figure 6. (b)

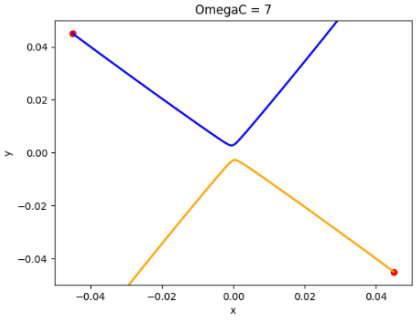

Figure 6. (c)

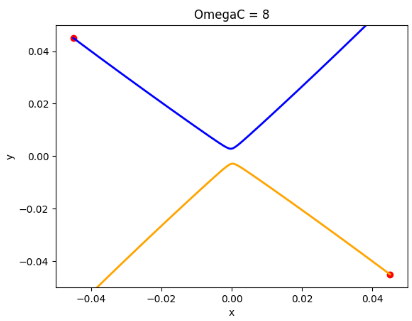

Figure 6. (d)

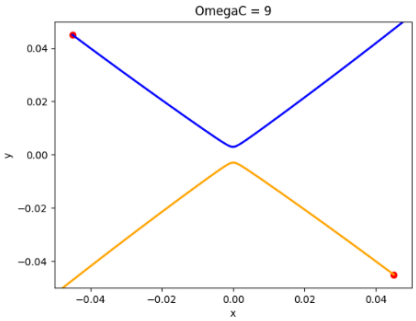

Figure 6. (e)

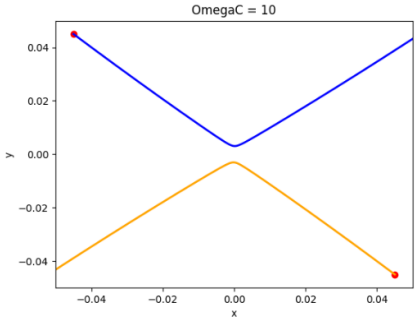

Figure 6. (f)

Figure 6. *As the cyclotron frequency is increased, the particles are more rotated away from their starting locations by the time they exit the constriction. Given the functionality and working of the Lorentz force, such a transformation is to be expected.*

For the purposes of this exploration, I will be assuming that each quadrant within the constriction represents a "detector"; in order to replicate consistent results with the experiment, the ωc = 9 trial provides with the most symmetrical results and will be used throughout the trials. While the position of the electrons will be slightly altered throughout the simulation in order to classically achieve the quantum effect of the 4 results, the velocities will be held constant throughout the experiment. If the electrons are given an initial velocity too high, they would travel an unnecessary distance within the constant finite difference ($dt = 0.00005$) and not interact with the electric potential and magnetic fields in a way similar to the real experiment due to the low resolution of points available to be plotted over the trial. However, if the electrons are given an initial velocity too low, the high resolution data would require a lot more computation and the resulting velocities will also be more influenced by the potentials than has been observed in the experiment which we are trying to replicate. In order to determine the most accurately representative velocity within the "factorized" version of this simulation, we plotted the trajectories of the electrons such that $v_{1x} = -v_{1y} = -v_{2x} = v_{2y}$, which means that the electrons are shot directly at each other with symmetrical velocities around the parameter $y = x$ within the constriction of our experiment. Below are some of the relevant simulations with the different values of v:

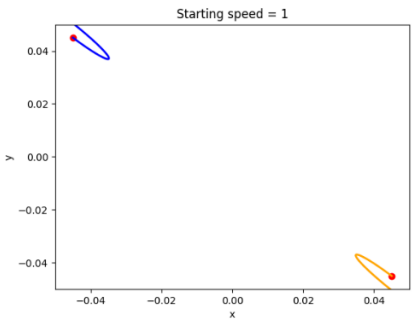

Figure 7. (a)

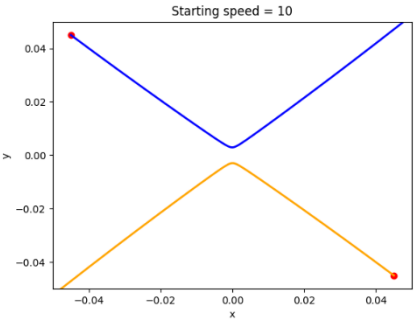

Figure 7. (b)

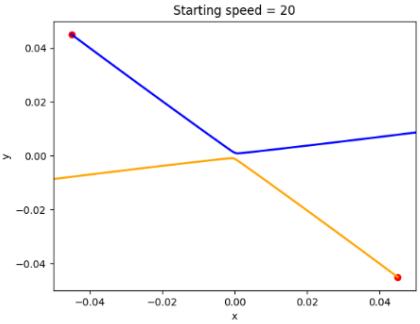

Figure 7. (c)

Figure 7. *As expected, the higher the velocity the lower the influence of the surrounding fields. As can be seen in the trajectories of the electrons starting with an initial velocity of 1 unit/sec; the overall coulomb collision and Lorentz interaction is much more prominent and take effect from an earlier time-stamp. As the initial velocities increase, the particles need to get much closer before an interaction is visible.*

With these interactions and trajectories in mind, it was decided that I will be holding a $v_{1x} = -v_{1y} = -v_{2x} = v_{2y} = 10$ as a constant throughout the trials and results.

4. Numerical results

Process of getting the figures and results

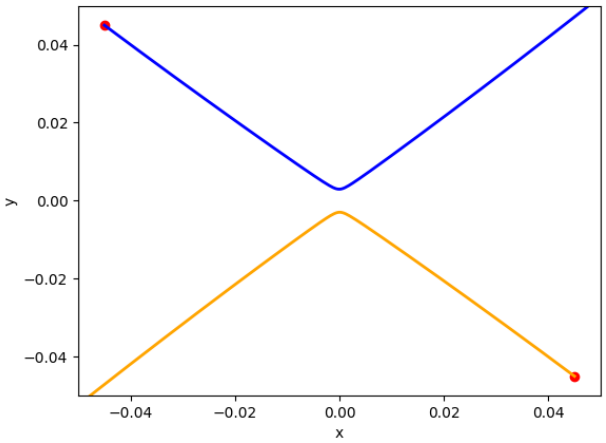

Figure 8. (a)

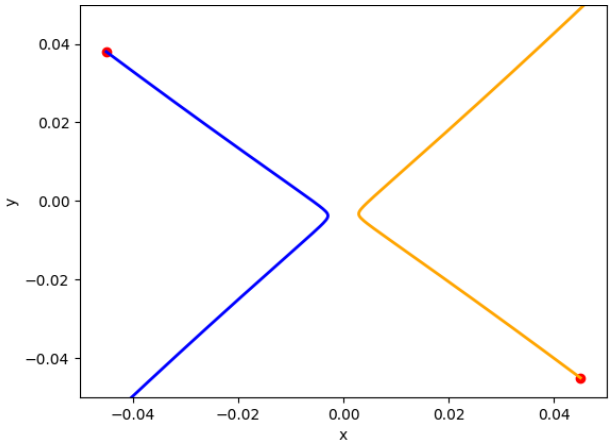

Figure 8. (b)

Figure 8. *(a) is the first of the 2 solutions calculated, representing as the 2 electrons going to separate detectors as they interact and has starting conditions as such: $\omega_y = \omega_x = 1$, $\omega_c = 9$, Starting positions: (0.045, -0.045), and (-0.045, 0.045). Fig.8(b) is the second of the 2 solutions, with the electrons still going to separate detectors, but each one going to a different one compared with (a) with the starting conditions as such: $\omega_y = \omega_x = 1$, $\omega_c = 9$, Starting positions: (0.045, -0.045), and (-0.045, 0.038)*

The detectors within a constriction like the one modelled throughout the report are placed in the location of the top-left and bottom-right quadrants with the expectation that the colliding electrons, just like the above trajectories demonstrate, will interact with one another and deflect back to one of the detectors (away from their starting quadrants). This was one out of the 4 possible outcomes as was elaborated in the experiment carried out by Dr. Ubbelohde [7]. Fig.8 (a) while being one of the most common outcomes (even in the reference papers), is still quite restricted in its possible ways to occur. If the constants are held as has been discussed in 3.2, and only the starting location of one of the electrons is altered, the result is only valid for co-ordinates $0.043 < y \leq 0.045$, x = -0.045 (for electron 1 (blue)) and $-0.045 \leq y < -0.043$, x = 0.045 (for electron 2 (yellow)) (Note: These values are to 2 significant figures). If the x-values remain constant, any deviation to the y-coordinate outside the inequality to the degree of 10^{-3} will not produce the desirable results. Fig.8 (b) was the second out of the 4 possible outcomes as was elaborated in the experiment. This, according to their experiment, was also one of the more common outcomes, however is still quite restricted in its possible ways to occur within our model. If the constants are held as have been in 3.2, and only the starting locations of one of the electrons is altered, the result is only valid for co-ordinates $0.033 < y \leq 0.038$, x = -0.045 (for electron 1 (blue)) and $-0.038 \leq y < 0.033$, x = 0.045 (for electron 2 (yellow)) (Note: These values are to 2 significant figures). If the x-values remain constant, any deviation to the y-coordinate outside the inequality to the degree of 10^{-3} will not produce the desirable results. Notice, however, that this result is possible in a much larger boundary than 4.1; where the inequality only existed between a value differences of 0.002, however this result exists between an inequality boundaries of 0.005.

Aside from the 2 results which have been parameterized and shown to function above, there are 2 other results which haven't been replicated. If we are to characterize the detection of an electron at the bottom left and top right detectors as (bottom left, top right), the following results: (2,0) and (0,2) are the results still remaining to be modeled on this classical simulation. Despite various personal attempts at modelling even those outcomes, we have not been able to exactly do so within this classical framework. While the 2 results might potentially be a consequence of the real world quantum interferences and interactions taking place, there may still be a way to achieve those results. The attempts at creating those remaining two results with our model utilized not only basic parameters like initial position and velocity, but also other parameters such as a softening factor and time-delay. The softening factor is modelling the screening effect of the medium on travelling electrons within the constriction while the time-delay is a physical implementation of a possible delay between the releases of the electrons from the initial positions.

The softening factor has a very clear influence on the trajectories of the electrons, where increasing the softening factor directly reduces the strength of the coulomb interaction between the particles. This physically occurs because the screening effect which is trying to be modelled is caused by the coulomb interaction between our target charged particle and the surrounding atoms. Due to the fact that beam splitters and other equivalent machinery are effectively influencing and directing particles the size of its own component material or even smaller, the atoms inside the medium and surroundings is something which cannot be assumed to not exist. Therefore, this particular phenomenon was modelled as a component to the coulomb interaction as $S_{screening}$ in (2) and *softening* in 7.1.

The time delay also introduces interesting variation to the trajectory of the electrons. Captured as the time_gap in 7.1, the gap allows one of the electrons (orange) to travel a certain distance before interacting with the other electron. However, it is to be noted that the way it is programmed, the non-delayed electron will still have a coulomb interaction with the stationary electron – mimicking how a restriction on a particle of such size would play out in real life.

5. Conclusion

This study has delved into the dynamics of electron collisions within a saddle-shaped electric potential and a constant magnetic field, resembling the conditions found in beam splitters and particle accelerators. While conventional research often employs a quantum framework for modeling and experimentation, our approach has been primarily classical – providing a more intuitive understanding of these interactions. By transitioning from quantum to classical representation, we have removed probabilistic elements, enabling precise and deterministic simulations.

Our efforts have resulted in the development of a Python script based on the mathematical expressions detailed in this paper. We successfully replicated 2 out of 4 expected results by simply altering the initial positions of the electrons. Furthermore, we have expanded the capabilities of our Python simulations to facilitate additional research and development. Specifically, we introduced a softening factor that governs the relative screening effect of the constriction material and a time delay feature to offset the starting times of the particles. Utilizing these two added factors, a large variation of new results can be mapped out, not to mention the variation which can be introduced within the constants, positions, and velocities themselves. Therefore, it is not unreasonable to assume that a method to derive the last two results become possible all within a classical framework.

Our aim with this paper is to provide a platform for the scientific community to access and utilize our findings, as well as the model we have employed to derive them. We hope that researchers will leverage this work for further exploration and advancement in the field of electron collisions and related applications in modern physics.

References

[1] Märk, Tilmann D., and Gordon H. Dunn, eds. Electron impact ionization. Springer Science & Business Media, 2013.

[2] Kiani, Farzad, and Fatih Copuroglu. "QUANTUM COMPUTING VS COMPUTERS COMPUTING." Research Journal of Computer Science 5: 236 - 240.

[3] Bretagne, J., J. Godart, and V. Puech. "Low-energy electron distribution in an electron-beam-generated argon plasma." Journal of Physics D: Applied Physics 15.11 (1982): 2205.

[4] Bouchiha, D., et al. "Low-energy electron collisions with tetrahydrofuran." Journal of Physics B: Atomic, Molecular and Optical Physics 39.4 (2006): 975.

[5] Hotop, H., et al. "Resonance and threshold phenomena in low-energy electron collisions with molecules and clusters." Advances in atomic, molecular, and optical physics. Vol. 49. Academic Press, 2003. 85 - 216.

[6] Yamabe, C., S. J. Buckman, and A. V. Phelps. "Measurement of free-free emission from low-energy-electron collisions with Ar." Physical Review A 27.3 (1983): 1345.

[7] Ubbelohde, Niels, et al. "Two electrons interacting at a mesoscopic beam splitter." Nature Nanotechnology (2023): 1-8.

[8] Monzon, Lorena MA, and John Michael David Coey. "Magnetic fields in electrochemistry: The Lorentz force. A mini-review." Electrochemistry Communications 42 (2014): 38 - 41.

[9] Fletcher, J. D., et al. "Time-resolved Coulomb collision of single electrons." Nature Nanotechnology (2023): 1 - 6.

[10] Michaud, André. "Demystifying the Lorentz Force Equation." Journal of Modern Physics 13.5 (2022): 776 - 838.

[11] Jones, W. P., and G. P. A. Berg. "Design of a beam transport system for a proton radiation therapy facility." Proceedings of the 1999 Particle Accelerator Conference (Cat. No. 99CH36366). Vol. 4. IEEE, 1999.

[12] Nielsen, T., et al. "High efficiency beam splitter for multifocal multiphoton microscopy." Journal of microscopy 201.3 (2001): 368 - 376.

[13] Lu, Cheng, and R. H. Lipson. "Interference lithography: a powerful tool for fabricating periodic structures." Laser & Photonics Reviews 4.4 (2010): 568 - 580.

[14] Pavlovska, Elina, et al. "Collision of two interacting electrons on a mesoscopic beam splitter: Exact solution in the classical limit." Physical Review B 107.16 (2023): 165304.

[15] Linge, Svein, and Hans Petter Langtangen. Programming for computations-Python: A gentle introduction to numerical simulations with Python 3.6. Springer Nature, 2020.

Appendix

Main Simulation

```
import numpy as np
import matplotlib.pyplot as plt

## Starting Position
ONEstartx = 0.045
ONEstarty = 0.045
velocity = 10
x_1 = [-ONEstartx]
y_1 = [ONEstarty]
x_2 = [0.045]
y_2 =[-0.045]

## Velocities
v_x1 = [velocity]
v_y1 = [-velocity]

v_x2 = [-velocity]
v_y2 = [velocity]
## This dictates the time-step, and number of computations

dt = 0.00005
N = 10000

## Physical Constants
omegaX = 1 ## Note -- Includes Ex and Ey
omegaY = 1 ## Note -- Includes Ex and Ey
omegaC = 9# Magnitude of Magnetic Field in z direction
```

```
e = -1 # Charge of electron
softening = 0 #Softening factor
time_gap = 0 # Time gap between the release of electron 2 and 1

## Defining the velocity Functions (If needed)

# Particle 1

def v1x (x1,x2,y1,y2,vx,vy):
    coulomb_effect = ((e**2*(x1-x2))*((x1-x2)**2+(y1-y2)**2+softening**2)**(-1.5))

    return dt*(omegaX**2*x1 + coulomb_effect + (e*vy*omegaC))+ vx

def v1y (x1,x2,y1,y2,vx,vy):
    coulomb_effect = ((e**2*(y1-y2))*((x1-x2)**2+(y1-y2)**2+softening**2)**(-1.5))

    return dt*(-omegaY**2*y1 + coulomb_effect - (e*vx*omegaC))+ vy

# Particle 2

def v2x (x1,x2,y1,y2,vx,vy):
    coulomb_effect = ((e**2*(x1-x2))*((x1-x2)**2+(y1-y2)**2+softening**2)**(-1.5))

    return dt*(omegaX**2*x2 - coulomb_effect + (e*vy*omegaC))+ vx

def v2y (x1,x2,y1,y2,vx,vy):
    coulomb_effect = ((e**2*(y1-y2))*((x1-x2)**2+(y1-y2)**2+softening**2)**(-1.5))

    return dt*(-omegaY**2*y2 - coulomb_effect - (e*vx*omegaC))+ vy

## Making the loop
    # i is our counting variable
    # N is our initially defined number of computations

for i in range (N):

    ## Solving for the velocities and storing values in a list

    #Particle 2

    v_x2.append(v2x(x_1[i],x_2[i],y_1[i],y_2[i],v_x2[i],v_y2[i]))
    v_y2.append(v2y(x_1[i],x_2[i],y_1[i],y_2[i],v_x2[i],v_y2[i]))

    ## Using velocities to calculate position and storing values in a list

    ##Time gap

    if i*dt < time_gap:

        v_x1[i] = 0
        v_y1[i] = 0
        v_x1.append(0)
        v_y1.append(0)
        x_1.append(-ONEstartx)
        y_1.append(ONEstarty)
    else:
        v_x1[round(time_gap/dt)] = velocity
        v_y1[round(time_gap/dt)] = -velocity
        v_x1.append(v1x(x_1[i],x_2[i],y_1[i],y_2[i],v_x1[i],v_y1[i]))
```

```
            v_y1.append(v1y(x_1[i],x_2[i],y_1[i],y_2[i],v_x1[i],v_y1[i]))
            x_1.append(v_x1[i+1]*dt + x_1[i])
            y_1.append(v_y1[i+1]*dt + y_1[i])

        ### round(time_gap/dt) gives an approximate value of i

    #Particle 2

        x_2.append(v_x2[i+1]*dt + x_2[i])
        y_2.append(v_y2[i+1]*dt + y_2[i])
    ## Plotting the positions in 2D

    bound = 0.05 ## I have made it just slightly wider than our inital position

    ## Setting up an axes for the plot

    plt.xlabel('x')
    plt.ylabel('y')
    #plt.title('Starting speed = ' + str(velocity))
    plt.xlim([-bound,bound])
    plt.ylim([-bound,bound])

        #Making a line for particle 1:

    plt.plot(x_1,y_1, color = 'blue', label = 'Particle 1', lw=2)
    plt.scatter(x_1[0], y_1[0] , c='red')

        #Making a line for particle 2:
    plt.plot(x_2,y_2, color = 'orange', label = 'Particle 2', lw=2)
    plt.scatter(x_2[0], y_2[0] , c='red')
    plt.plot(x_1[0],y_1[0])

    ## Making the graphs visible
    plt.show()
```